

# Meson-Hybrid Mixing in Vector ( $1^-$ ) and Axial Vector ( $1^{++}$ ) Charmonium

D. Harnett, A. Palameta, J. Ho, and T. G. Steele

## Introduction

Hybrid mesons contain a constituent quark, antiquark, and gluon. They have not yet been conclusively observed. Hadron mixing, the idea that hadrons are superpositions of “pure” states (e.g.,  $q\bar{q}$ -mesons and hybrids), might be hampering hybrid detection and/or identification.

To explore this idea, we look to the XYZ resonances [1], a set of charmonium-like states many of which are not readily interpreted as  $q\bar{q}$ -mesons. Specifically, we focus on the vector ( $1^-$ ) and axial vector ( $1^{++}$ ) channels. The known resonances in these channels [2] are depicted in Figure 1.

We test the resonances of Figure 1 for coupling to a meson-hybrid cross-correlator using QCD sum-rules. QCD sum-rules are transformed dispersion relations that relate QCD-calculated correlators to hadronic spectral functions [3, 4]. We use measured resonance masses as input to the hadronic spectral function, and extract products of meson and hybrid couplings (i.e., mixing parameters) as best-fit parameters between QCD and hadron physics. Resonances with non-zero mixing parameters can be interpreted as having both meson and hybrid components.

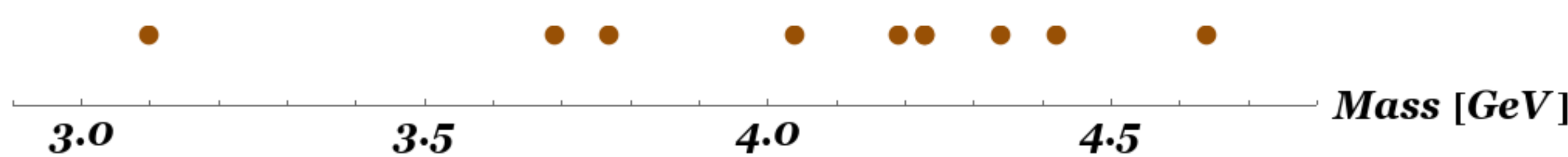


Figure 1: Observed spin-1 charmonium-like resonances. The upper dots represent vector ( $1^-$ ) states; the lower dots represent axial vector ( $1^{++}$ ) states.

## Currents and Correlators

Consider the (momentum-space) charmonium meson-hybrid cross-correlator

$$\Pi(Q^2) = \frac{i}{D-1} \left( \frac{q_\mu q_\nu}{q^2} - g_{\mu\nu} \right) \int d^D x e^{iq \cdot x} \langle \Omega | \tau j_\mu^{(m)}(x) j_\nu^{(h)}(0) | \Omega \rangle, \quad Q^2 = -q^2$$

where  $D=4+2\epsilon$  is spacetime dimension and  $j^{(m)}$  and  $j^{(h)}$  are respectively meson and hybrid currents,

$$j_\mu^{(m)} = \begin{cases} \bar{c} \gamma_\mu c & \text{for } 1^{--} \\ \bar{c} \gamma_\mu \gamma_5 c & \text{for } 1^{++} \end{cases} \quad \text{and} \quad j_\nu^{(h)} = \begin{cases} g_s \bar{c} \gamma^\rho \gamma_5 \frac{\lambda^a}{2} \left( \frac{1}{2} \epsilon_{\nu\rho\omega\eta} G_{\omega\eta}^a \right) c & \text{for } 1^{--} \\ g_s \bar{c} \gamma^\rho \frac{\lambda^a}{2} \left( \frac{1}{2} \epsilon_{\nu\rho\omega\eta} G_{\omega\eta}^a \right) c & \text{for } 1^{++} \end{cases}$$

for charm quark  $c$ , gluon field strength  $G_{\omega\eta}^a$ , and Levi-Civita symbol  $\epsilon_{\nu\rho\omega\eta}$ . We compute  $\Pi(Q^2)$  to leading-order in  $g_s$  using the operator product expansion (OPE) in which perturbation theory is corrected by non-perturbative condensate terms. We take into account condensates of dimension-six (6d) or less. Corresponding diagrams are shown in Figure 2. Results, omitted here for brevity, are in [5, 6].

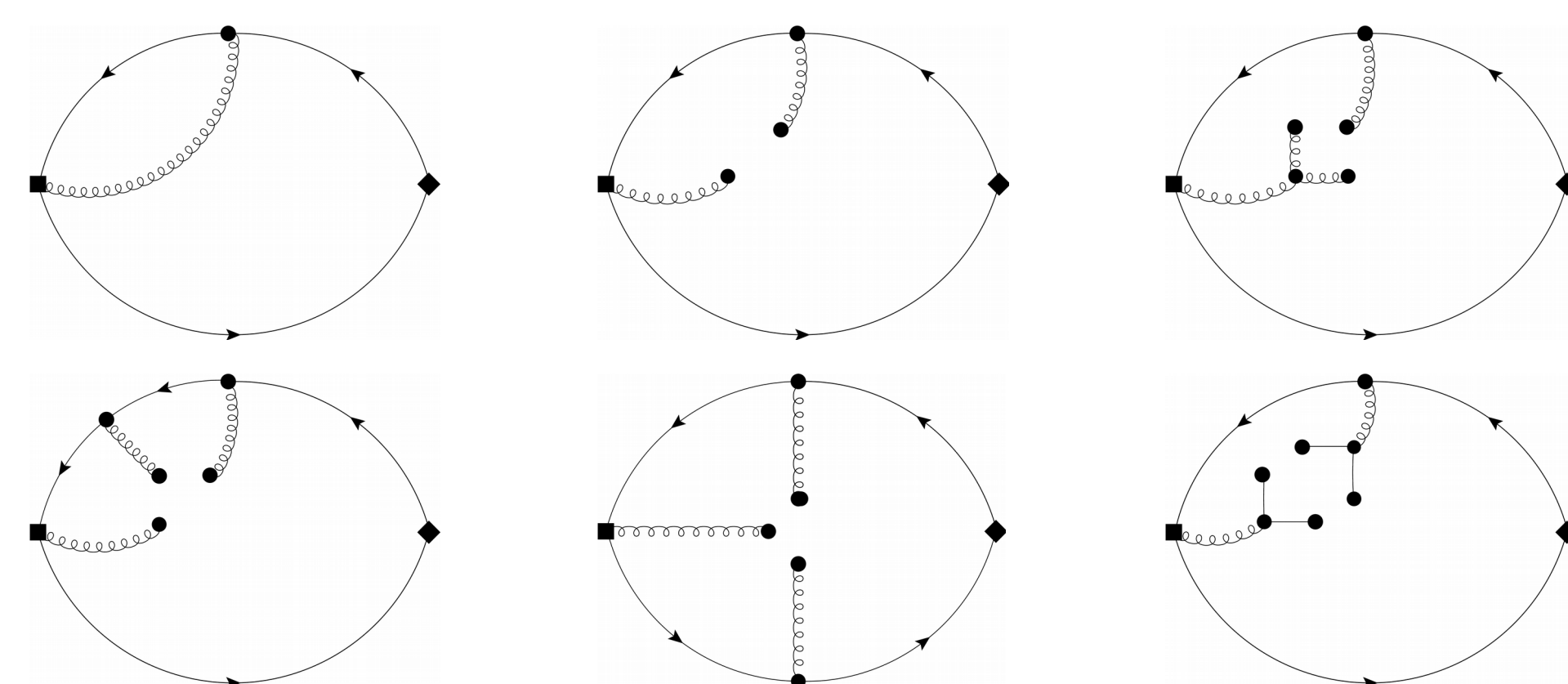


Figure 2: Diagrams computed for the cross-correlator  $\Pi(Q^2)$ . Square vertices are hybrid currents; diamond vertices are meson currents. The upper-left diagram is perturbation theory. The others are non-perturbative corrections due to the 4d and 6d gluon condensates and the 6d quark condensate.

Perturbation theory contains a non-local divergence eliminated by letting  $j^{(h)}$  mix under renormalization:

$$j_\nu^{(h)} \rightarrow j_\nu^{(h)} - \frac{5g_s^2 m^2}{18\pi^2 \epsilon} \bar{c} \gamma_\nu c + \frac{g_s^2 m}{9\pi^2 \epsilon} \bar{c} i D_\nu c \quad \text{for } 1^{--},$$

$$j_\nu^{(h)} \rightarrow j_\nu^{(h)} - \frac{5g_s^2 m^2}{18\pi^2 \epsilon} \bar{c} \gamma_\nu \gamma_5 c - \frac{g_s^2 m}{9\pi^2 \epsilon} \bar{c} i \gamma_5 D_\nu c \quad \text{for } 1^{++}.$$

This leads to the two renormalization-induced diagrams shown in Figure 3. Final results for the renormalized cross-correlator, (again) omitted for brevity, are in [5, 6].

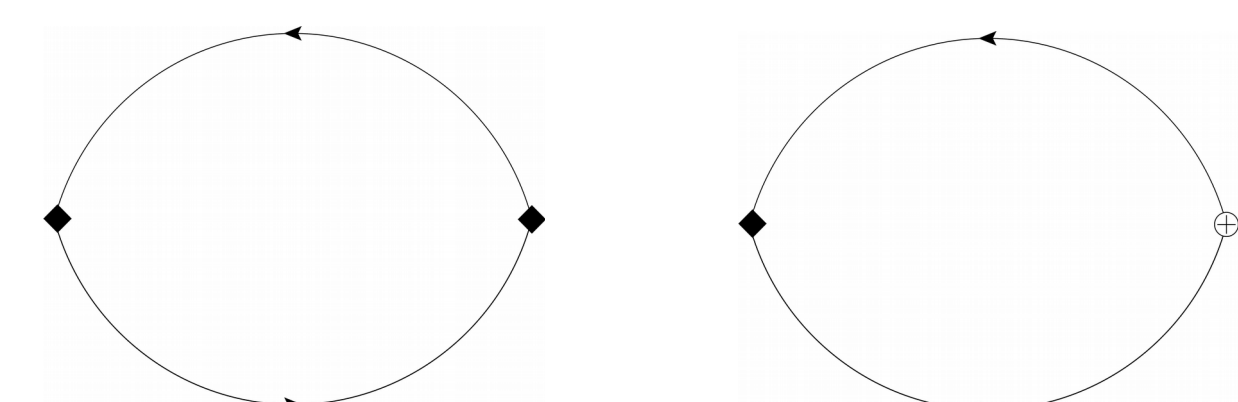


Figure 3: Renormalization-induced diagrams. Diamond vertices are meson currents. The “+” vertex is a derivative current.

## Analysis Methodology

We use a resonance(s)-plus-continuum decomposition of the hadronic spectral function,

$$\frac{1}{\pi} \text{Im}\Pi(t) = \rho^{\text{had}}(t) + \frac{1}{\pi} \text{Im}\Pi^{\text{OPE}}(t) \Theta(t - s_0),$$

where  $\Theta(t-s_0)$  is a step function at continuum threshold parameter  $s_0$ . The resonance content,  $\rho^{\text{had}}(t)$ , is modelled as a sum of narrow resonances

$$\rho^{\text{had}}(t) = \sum_{i=1}^n \xi_i \delta(t - m_i^2)$$

where  $m_i$  are resonance masses and  $\xi_i$  are mixing parameters. **A nonzero mixing parameter indicates coupling to both meson and hybrid currents.** Specific models and their corresponding resonance masses are defined in Tables 1 & 2 for  $1^-$  and  $1^{++}$  channels respectively. In the  $1^-$  channel, densely packed resonances are amalgamated as single effective resonances.

QCD Laplace sum-rules,  $\mathcal{R}(\tau)$ , are defined in terms of transformed correlation functions

$$\mathcal{R}(\tau) = \frac{1}{\tau} \lim_{\substack{N, Q^2 \rightarrow \infty \\ \tau = N/Q^2}} \frac{(-Q^2)^N}{\Gamma(N)} \left( \frac{d}{dQ^2} \right)^N \Pi(Q^2)$$

$$= \int_0^{s_0} e^{-t\tau} \rho^{\text{had}}(t) dt + \int_{s_0}^{\infty} e^{-t\tau} \frac{1}{\pi} \text{Im}\Pi^{\text{OPE}}(t) dt$$

where  $\tau$  is the Borel scale. For each of the models in Tables 1 & 2,  $s_0$  and  $\xi_i$  are determined as best fit parameters to the Laplace sum-rules over an acceptable Borel window ( $\tau_{\min}, \tau_{\max}$ ). Results are given in Tables 3 & 4, and plots of relative residuals are shown in Figures 5 & 6.

Table 1: Hadron masses ( $m_i$ ) of the  $1^-$  models. Model V4 has a nonzero width for the heaviest resonance (i.e.,  $\Gamma_3$ ).

Model	$m_1$ [GeV]	$m_2$ [GeV]	$m_3$ [GeV]	$\Gamma_3$ [GeV]
V1	3.10	–	–	–
V2	3.10	3.73	–	–
V3	3.10	3.73	4.30	–
V4	3.10	3.73	4.30	0.30

Table 2: Hadron masses ( $m_i$ ) of the  $1^{++}$  models.

Model	$m_1$ [GeV]	$m_2$ [GeV]	$m_3$ [GeV]	$m_4$ [GeV]
A1	3.51	–	–	–
A2	3.51	3.87	–	–
A3	3.51	3.87	4.15	–
A4	3.51	3.87	4.15	4.27

## Results

Table 3: Continuum thresholds ( $s_0$ ), chi-squares ( $\chi^2$ ) relative to Model V1, and scaled mixing parameters ( $\xi_i/\zeta$ ) where  $\zeta = \sum |\xi_i|$  for the  $1^-$  hadron models of Table 1.

Model	$s_0$ [GeV <sup>2</sup> ]	$\frac{\chi^2}{\chi^2[\text{V1}]}$	$\zeta$ [GeV <sup>6</sup> ]	$\frac{\xi_1}{\zeta}$	$\frac{\xi_2}{\zeta}$	$\frac{\xi_3}{\zeta}$
V1	12.5	1	0.51(2)	1	–	–
V2	13.9	0.73	0.73(4)	0.72(3)	0.27(3)	–
V3	24.1	0.038	2.9(4)	0.22(1)	–0.02(5)	0.76(3)
V4	24.2	0.038	3.0(3)	0.21(1)	–0.03(5)	0.76(3)

Table 4: The same as Table 3 but for the  $1^{++}$  hadron models.

Model	$s_0$ [GeV <sup>2</sup> ]	$\frac{\chi^2}{\chi^2[\text{A1}]}$	$\zeta$ [GeV <sup>6</sup> ]	$\frac{\xi_1}{\zeta}$	$\frac{\xi_2}{\zeta}$	$\frac{\xi_3}{\zeta}$	$\frac{\xi_4}{\zeta}$
A1	18.8	1	0.18(1)	1	–	–	–
A2	28.8	0.0095	0.83(7)	0.47(2)	–0.53(2)	–	–
A3	18.8	0.0034	2.6(4)	0.21(2)	–0.45(1)	0.34(2)	–
A4	31.7	$7.3 \times 10^{-6}$	44(6)	0.03(1)	–0.16(1)	0.46(1)	–0.35(1)

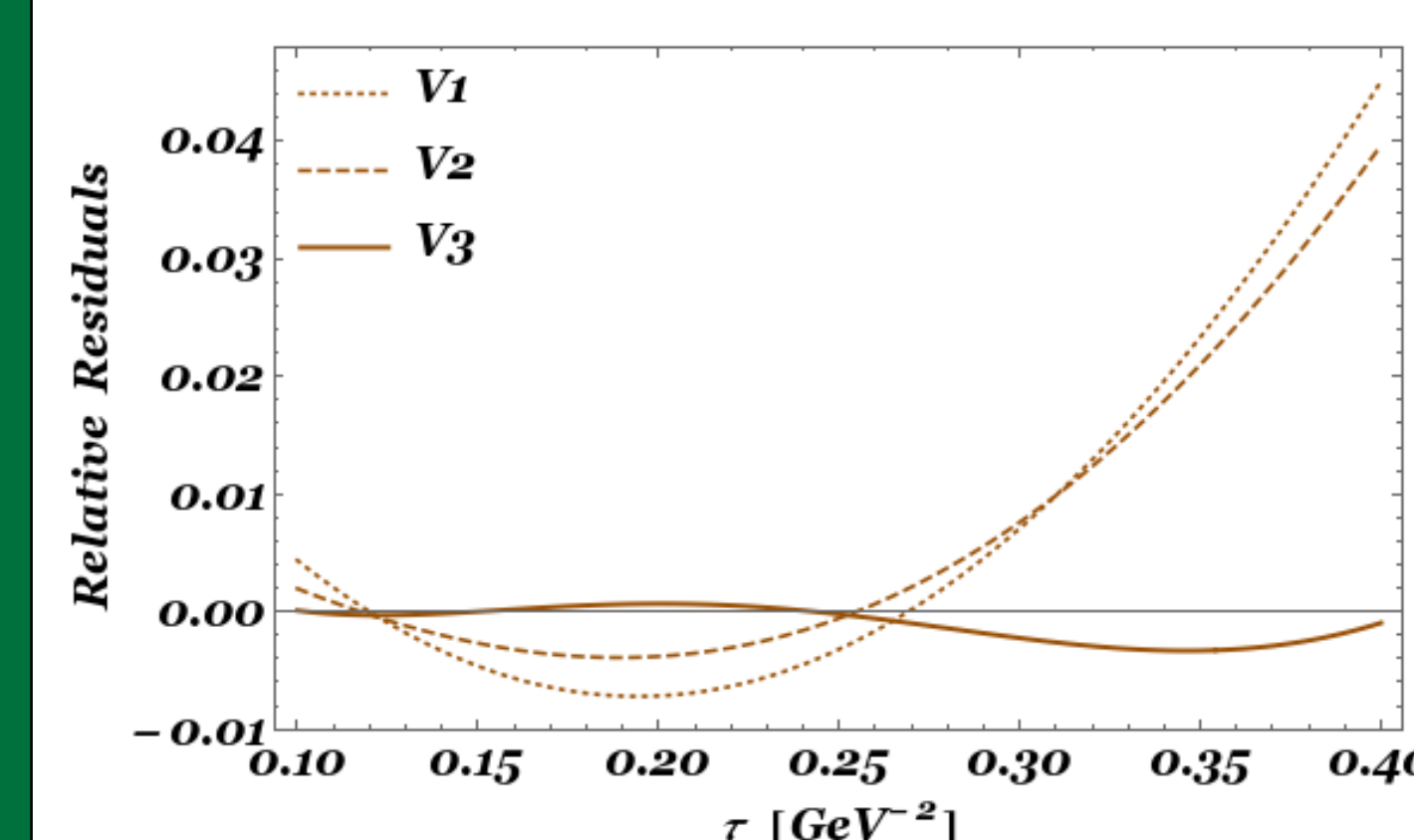


Figure 5: Relative residuals of the QCD sum-rules  $\mathcal{R}(\tau)$  for a selection of the  $1^-$  hadron model results of Table 3.

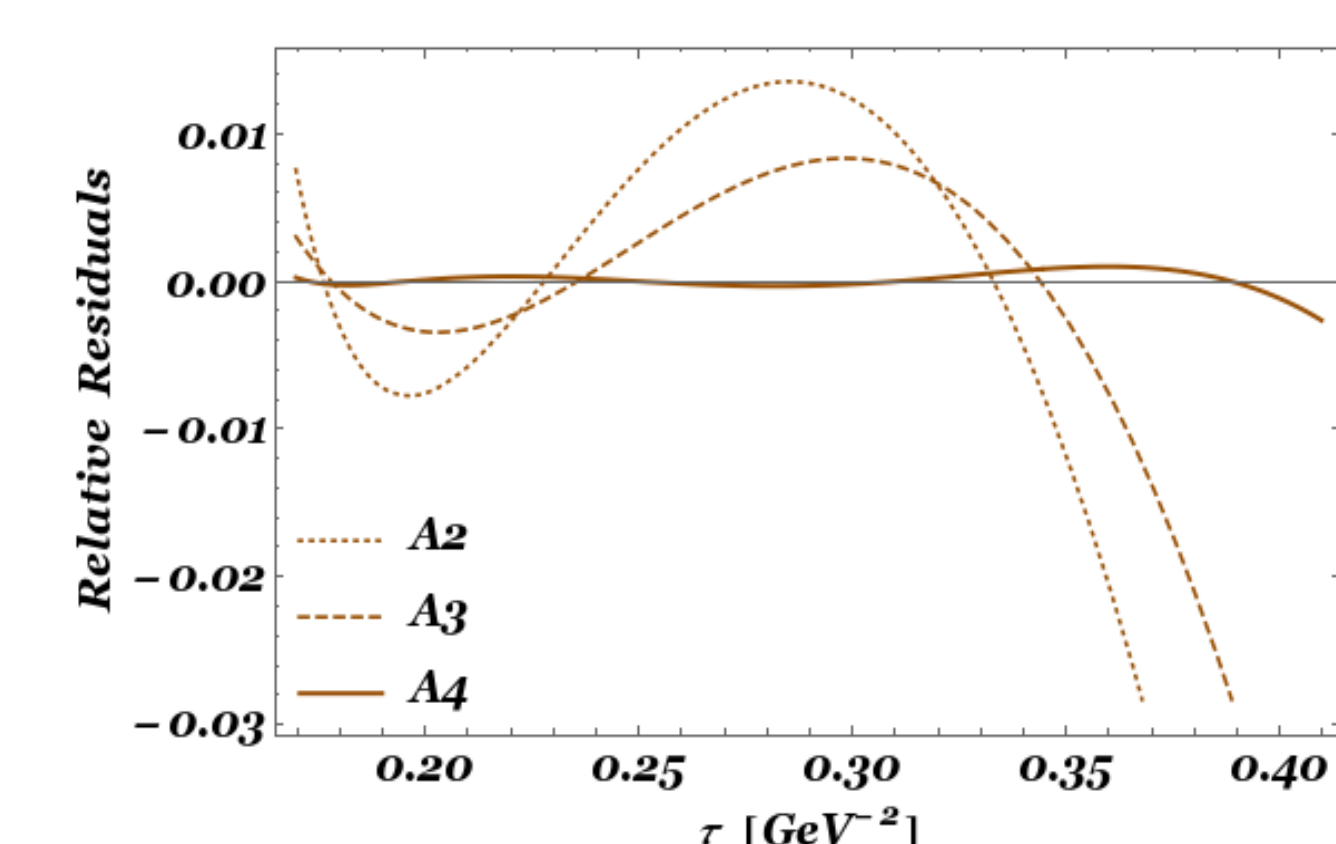


Figure 6: The same as Figure 5 but for a selection of the  $1^{++}$  hadron model results of Table 4.

## Discussion

From the chi-squares columns of Tables 3 & 4, we see that agreement between theoretically calculated QCD Laplace sum-rules and hadron physics is significantly improved by including both excited resonances and the ground state in the hadron model. Based on chi-squares values, we favour either Model V3 or V4 in the  $1^-$  channel and Model A4 in the  $1^{++}$  channel. Note that the difference between Models V3 and V4 is a nonzero width on the 4.3 GeV resonance. Laplace sum-rules are generally insensitive to symmetric resonance widths, and so it is unsurprising that our analysis does not strongly distinguish between the two models.

By design, QCD Laplace sum-rules exponentially suppress contributions from heavy resonances relative to lighter ones, and so it is important to check that the heavy resonances of Models V3, V4, and A4 make numerically significant contributions. As a quantitative measure in, for example, Model V3, consider

$$\frac{|\xi_3| \int_{\tau_{\min}}^{\tau_{\max}} e^{-m_3^2 \tau} d\tau}{\sum_{i=1}^3 |\xi_i| \int_{\tau_{\min}}^{\tau_{\max}} e^{-m_i^2 \tau} d\tau},$$

i.e., the ratio of the heaviest resonance’s contribution to the sum-rules to the total resonance contribution to the sum-rules. Using values of  $m_i$  and  $\xi_i$  from Tables 1 and 3 respectively, this ratio evaluates to 0.43. In the  $1^{++}$  channel, an analogous ratio measuring the relative contribution to the sum-rules of  $m_4$  gives 0.25.

In the  $1^-$  channel, we find evidence for small meson-hybrid mixing in the  $J/\psi$ , no evidence for mixing in the  $\psi(2S)$  or  $\psi(3770)$ , and significant mixing around 4.3 GeV. These results are consistent with the  $J/\psi$  being predominantly a meson but with a small hybrid component. As for the heavier state, it has been speculated that the X(4260) has a significant hybrid component (see Ref. [7], for example), an interpretation consistent with our findings.

In the  $1^{++}$  channel, we find essentially no evidence for mixing in the ground state,  $\chi_{c1}(1P)$ , minimal mixing in the X(3872), and significant mixing in the X(4140) and the X(4274). Ref. [8] argues that the X(3872) has a large meson component while Ref. [9] argues that it has a large hybrid component. Our results are compatible with either conclusion, but not both.

## Conclusions

Employing QCD Laplace sum-rules, we explored meson-hybrid mixing in  $1^-$  and  $1^{++}$  charmonium. Using measured masses as inputs, we tested experimentally observed resonances for coupling to both meson and hybrid currents, i.e., for meson-hybrid mixing. In both channels, agreement between QCD and hadron physics was significantly improved by the inclusion of excited states in addition to the ground state. In the  $1^-$  channel, we found that meson-hybrid mixing can be described by a two resonance scenario consisting of the  $J/\psi$  and a 4.3 GeV state (perhaps the X(4260)). In the  $1^{++}$  channel, we found almost no mixing in the ground state,  $\chi_{c1}(1P)$ , minimal mixing in the X(3872), and significant mixing in both the X(4140) and X(4274).

## Acknowledgements

We are grateful for financial support from the National Sciences and Engineering Research Council of Canada.

## References

1. N. Brambilla *et al.*, Eur. Phys. J. **C71** (2011) 1534 [1010.5827].
2. Particle Data Group, C. Patrignani *et al.*, Chin. Phys. **C40** (2019) 100001.
3. M. A. Shifman, A. I. Vainshtein, and V. I. Zakharov, Nucl. Phys. **B147** (1979) 385.
4. M. A. Shifman, A. I. Vainshtein, and V. I. Zakharov, Nucl. Phys. **B147** (1979) 448.
5. A. Palameta, J. Ho, D. Harnett, and T.G. Steele, Phys. Rev. **D97** (2018) 034001 [1707.00063].
6. A. Palameta, D. Harnett, and T.G. Steele, Phys. Rev. **D98** (2018) 074014 [1805.04230].
7. S.-L. Zhu, Phys. Lett. **B631** (2005) 212 [hep-ph/0507025].
8. W. Chen *et al.*, Phys. Rev. **D88** (2013) 045027 [1305.0244].
9. R. D. Matheus *et al.*, Phys. Rev. **D80** (2009) 056002 [0907.2683].

